Sequence-Specific Recognition of DNA by Phenanthrenequinone Diimine Complexes of Rhodium(III): Importance of Steric and van der Waals Interactions†

Ayesha Sitlani and Jacqueline K. Barton*

Division of Chemistry and Chemical Engineering, California Institute of Technology, Pasadena, California 91125

Received May 27, 1994; Revised Manuscript Received July 20, 1994®

ABSTRACT: The importance of steric and van der Waals interactions in the sequence-specific recognition of DNA by $[Rh(phi)]^{3+}$ complexes has been explored through the synthesis and application of a series of $Rh(phi)^{3+}$ (phi: 9,10-phenanthrenequinone diimine) derivatives. $[Rh(phi)]^{3+}$ complexes intercalate in the major groove of DNA via the phi ligand and promote strand scission in the presence of UV light. The complexes reported here are derivatives of the parent molecules $[Rh(phi)_2bpy]^{3+}$ and $[Rh(bpy)_2phi]^{3+}$ (bpy: 2,2′-bipyridyl). The $[Rh(phi)]^{3+}$ complexes have comparable photoefficiencies; therefore, their different photocleavage patterns on ^{32}P-end-labeled DNA fragments reflect their unique sequence-specific recognition characteristics. The shapes of the $[Rh(phi)]^{3+}$ complexes are found to govern DNA recognition and reaction. Importantly and generally, the more sterically bulky complexes, containing methyl or phenyl groups on the ancillary ligands, cleave DNA at a *subset of sequences* recognized by their parent molecules. $[Rh(diphenylbpy)_2phi]^{3+}$ specifically targets the site 5′-CTCTAGAG-3′. Furthermore, chiral discrimination in site selectivity is observed; the different isomers target different sites. Δ- and Λ-$[Rh(5,5'\text{-dimethylbpy})_2phi]^{3+}$ cleave specifically at sites that are defined by the consensus sequences 5′-C-T-N-G-3′ and 5′-A-C/G-T-C/G-3′, respectively. The sequence selectivities may be understood on the basis of both negative steric clashes and positive van der Waals interactions between methyl groups on the metal complex and thymine methyl groups in the DNA major groove.

Our laboratory has focused on the design of transition metal complexes that site-specifically bind to nucleic acids (Pyle & Barton, 1990; Chow & Barton, 1992). These transition metal complexes have rigid, three-dimensional shapes owing to their restricted coordination geometries. Phenanthrenequinone diimine (phi) complexes designed in our laboratory have been shown to intercalate in the major groove of DNA (Pyle et al., 1989a,b; Sitlani et al., 1992; David & Barton, 1993; Krotz et al., 1993a). Intercalation by these coordination complexes therefore provides us with a well-defined and oriented scaffold on which to append moieties that may contribute to site-selective recognition. We have applied this strategy in the predictive design of Δ,α-(*R*,*R*)-$[Rh(Me_2trien)phi]^{3+}$ (phi: 9,10-phenanthrenequinone diimine; trien: triethylenetetramine), a metallointercalator that specifically targets the sequence 5′-TGCA-3′ through a mixture of hydrogen-bonding and van der Waals interactions in the major groove of DNA (Krotz et al., 1993b). The complex Δ-$[Rh(diphenylbpy)_2phi]^{3+}$ represents a remarkably sequence-selective molecule (Sitlani et al., 1993). This complex specifically targets the sequence 5′-CTCTAGAG-3′ through steric *shape-selective* interactions, as well as through noncovalent dimerization on the DNA helix. By systematically constructing a series of octahedral metal complexes with ligands containing different functionalities, here we explore some of the features that affect sequence-selective recognition.

The different DNA recognition characteristics of the complexes $[Rh(phen)_2phi]^{3+}$ and $[Rh(phi)_2bpy]^{3+}$, which are quite similar electronically, can be understood on the basis of shape selection, and they offer a starting point for systematic examination. Both complexes bind in the DNA major groove through intercalation of their phi ligand (David & Barton, 1993; Sitlani et al., 1992), which allows them to associate intimately with the helix and sense the local structure at that site. Upon photoactivation, both complexes promote DNA cleavage with comparable efficiency, which permits an assay of site-selective binding. However, these complexes display remarkably different DNA recognition characteristics from one another, based on subtle differences in their shapes. While $[Rh(phen)_2phi]^{3+}$ binds DNA sequence-selectively, $[Rh(phi)_2bpy]^{3+}$ is relatively sequence-neutral in its recognition of DNA (Pyle et al., 1989a; Sitlani et al., 1992). The selectivity of $[Rh(phen)_2phi]^{3+}$ for 5′-pyr-pyr-pur-3′ sites, which tend to be more open in the major groove, has been attributed to the steric clashes of the ancillary phenanthroline ligands at sites that are not somewhat opened; similar steric constraints are not evident with $[Rh(phi)_2bpy]^{3+}$.

Here we describe in detail the sequence-specific recognition of DNA by a series of $[Rh(phi)]^{3+}$ complexes (Figure 1), which are derivatives of the complexes $[Rh(phi)_2bpy]^{3+}$ and $[Rh(bpy)_2phi]^{3+}$. We find that the introducion of hydrophobic groups on the nonintercalating bipyridyl ligands of the complexes $[Rh(bpy)_2phi]^{3+}$ and $[Rh(phi)_2bpy]^{3+}$ increases the steric requirements for phi intercalation and enhances the overall specificity of these complexes for local DNA structure. In comparison, the hydrogen-bonding amido groups enhance the affinities, but not the specificities, of $[Rh(phi)]^{3+}$ complexes for DNA. Overall, then, the shapes of these complexes dominate their DNA recognition characteristics.

EXPERIMENTAL SECTION

Materials. 9,10-Diaminophenanthrene (DAP), 2,2′-bipyridyl (bpy), and 1,10-phenanthroline (phen) were purchased

†We are grateful to the National Institute of General Medical Sciences (GM33309) for financial support of this research.

* Author to whom correspondence should be addressed.

® Abstract published in *Advance ACS Abstracts,* September 1, 1994.

0006-2960/94/0433-12100$04.50/0

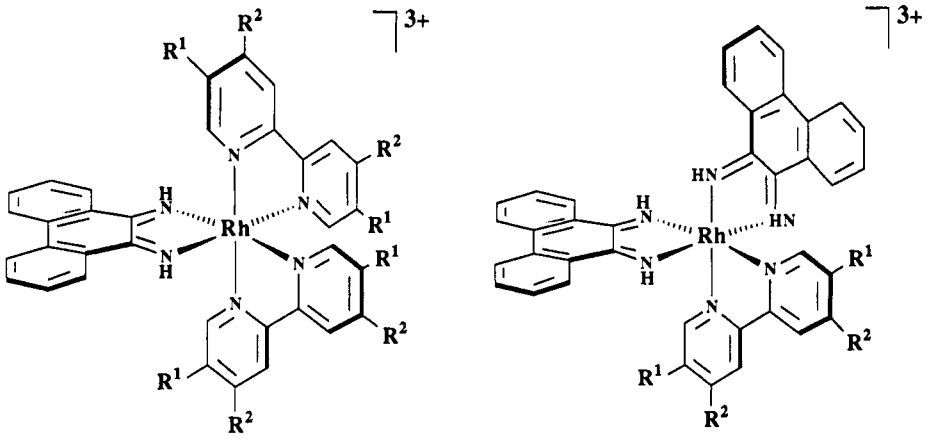

$R^1 = H, R^2 = H$
$R^1 = H, R^2 = phenyl$
$R^1 = H, R^2 = amido$
$R^1 = methyl, R^2 = H$

$R^1 = H, R^2 = H$
$R^1 = H, R^2 = phenyl$
$R^1 = H, R^2 = amido$
$R^1 = methyl, R^2 = H$

FIGURE 1: Structures of $[Rh(bpy)_2phi]^{3+}$ (left) and $[Rh(phi)_2bpy]^{3+}$ (right): bpy, 2,2′-bipyridine; phi, 9,10-phenanthrenequinone diimine. The complexes $[Rh(4,4'\text{-}R_2bpy)_2phi]^{3+}$ (R = phenyl or amido), $[Rh(5,5'\text{-}Me_2bpy)_2phi]^{3+}$, $[Rh(phen)_2phi]^{3+}$, $[Rh(4,4'\text{-}R_2bpy)(phi)_2]^{3+}$ (R = phenyl or amido), $[Rh(5,5'\text{-}Me_2bpy)(phi)_2]^{3+}$, and $[Rh(phen)(phi)_2]^{3+}$ were used in this study.

from Aldrich, and 4,4′-diphenylbipyridyl and 4,4′-dicarboxy-2,2′-bipyridyl were purchased from GFS Chemicals. $RhCl_3 \cdot 6H_2O$ was purchased from Aesar Johnson-Matthey. 5,5′-Dimethyl-2,2′-bipyridyl was synthesized as described previously (Badger & Sasse, 1956). The ligand 4,4′-diamido-2,2′-bipyridyl was synthesized from 4,4′-dicarboxy-2,2′-bipyridyl. The dicarboxy derivative was converted to the acyl halide using thionyl chloride, as described in the literature (Evers & Moore, 1986). The acyl halide was then dissolved in dry CH_2Cl_2, and NH_3 gas was bubbled through to generate the white, precipitated amide product. Calf thymus DNA was purchased from Sigma, and plasmid pUC18 was purchased from Boehringer-Mannheim. Phosphoramidites and solid supports for oligonucleotide synthesis were obtained from Pharmacia. All enzymes utilized were from commercial sources. [α-^{32}P]Dideoxy-ATP was obtained from Amersham, and [α-^{32}P]deoxy-ATP and [γ-^{32}P]deoxy-ATP were obtained from NEN-DuPont.

Instrumentation. ^{1}H NMR spectra were obtained on a JEOL GX-400 spectrometer or on a General Electric QE-300 spectrometer in D_2O (referenced to 4.65 ppm), CD_3OD (referenced to 4.78 ppm), or DMSO-d_6 (referenced to 2.49 ppm). UV–visible spectra and circular dichroism spectra were recorded on a Cary 2200 spectrophotometer and on a JASCO J-500A spectropolarimeter, respectively, in 50 mM sodium cacodylate buffer (pH 7.0). The light source utilized in all photocleavage experiments was an Oriel Model 6140, 1000 W Hg/Xe lamp fitted with a monochromator and a 300 nm cutoff filter to avoid light damage to DNA. High-performance liquid chromatography (HPLC) was performed on a Waters 600E system equipped with a 484 tunable detector. Autoradiograms were scanned with an LKB 2202 Ultrascan laser densitometer.

Synthesis. A. [Rh(phi)$_2$bpy]Cl$_3$ and Derivatives. The complex $[Rh(phi)_2bpy]Cl_3$ and its derivatives $[Rh(phi)_2(4,4'\text{-}R_2bpy)]Cl_3$ (R = phenyl or amido), $[Rh(phi)_2(5,5'\text{-}Me_2bpy)]Cl_3$, and $[Rh(phi)_2phen]Cl_3$, as shown in Figure 1, were prepared by a modified synthesis of $[Rh(phi)_2bpy]Cl_3$ (Pyle et al., 1990a). In this altered method, the precursor complex $[Rh(phi)_2Cl_2]Cl$ was first converted to $[Rh(phi)_2(H_2O)_2](OSO_2CF_3)_3$ by standard methods (Howells & McCown, 1977), before the addition of the 2,2′-bipyridyl-like ligand, to form the desired product complex. A mixture of $[Rh(phi)_2Cl_2]Cl$ (50 mg, 0.08 mmol) and $Ag(OSO_2CF_3)$ (72 mg, 0.28 mmol) was suspended in 50 mL of DMF/H_2O (5:1) and stirred overnight in the dark at room temperature. The milky solution was then centrifuged to pellet out the insoluble AgCl formed during the reaction. The supernatant, containing the intermediate complex $[Rh(phi)_2(H_2O)_2](OSO_2CF_3)_3$, was evaporated to dryness and then washed with water to remove unreacted $Ag(OSO_2CF_3)$. The complex $[Rh(phi)_2(H_2O)_2](OSO_2CF_3)_3$ (50 mg) and the appropriate bipyridyl ligand in a 1:1.2 molar ratio were dissolved in 75 mL of DMF and reacted at 60 °C for 2 h. The reaction was then brought to dryness and the product was extracted into water. The aqueous solution was then subjected to chloroform and ether extractions to remove unreacted ligands and impurities. The triflate salts of the product complexes were converted into the corresponding chloride salts by anion-exchange chromatography (QAE-Sephadex). Each product complex was purified on a C-18 column using a 1:1 methanol/water mixture as the eluent. The spectral data for the characterization of $[Rh(phi)_2bpy]Cl_3$ have been previously reported (Pyle et al., 1990a); characteristic data for its derivative complexes are described here.

[Rh(phi)$_2$(4,4′-diphenyl-2,2′-bipyridyl)]Cl$_3$: ^{1}H NMR (DMSO) δ 13.94 (s, 2 H), 13.57 (s, 2 H), 9.42 (s, 2 H), 8.68 (m, 4 H), 8.60 (d, 4 H), 8.49 (d, 4 H), 8.25 (d, 2 H), 8.15 (d, 4 H), 7.86 (d, 4 H), 7.67 (m, 10 H); FABMS 823 ($[Rh(phi)_2(diphenylbpy)]^+$), 617 ($[Rh(phi)(diphenylbpy)]^+$), 515 ($[Rh(phi)_2]^+$); extinction coefficient (ϵ) at λ = 350 nm, 19 400 M^{-1} cm^{-1}. Anal. Calcd (Found) for $[Rh(phi)_2(4,4'\text{-diphenylbpy})]Cl_3 \cdot 6H_2O$: C, 57.83 (58.1); H, 4.67 (4.5); N, 8.10 (7.8).

[Rh(phi)$_2$(4,4′-diamido-2,2′-bipyridyl]Cl$_3$: ^{1}H NMR (DMSO) δ 14.13 (s, 2 H), 13.56 (s, 2 H), 9.56 (s, 2 H), 8.84

(m, 4 H), 8.63 (s, 4 H), 8.48 (d, 4 H), 8.30 (m, 2 H), 8.21 (d, 2 H), 7.85 (d, 4 H), 7.63 (m, 4 H); FABMS 756 ([Rh(phi)$_2$(4,4′-diamidobpy)]$^+$), 551 ([Rh(phi)(4,4′-diamidobpy)]$^+$), 515 [Rh(phi)$_2$]$^+$; extinction coefficient (ϵ) at λ = 350 nm, 18 000 M^{-1} cm^{-1}. Anal. Calcd (Found) for [Rh(phi)$_2$(4,4′-diamidobpy)]Cl$_3$·12H$_2$O: C, 44.47 (43.8); N, 10.38 (9.8); H, 5.05 (4.90).

[Rh(phi)$_2$(5,5′-dimethyl-2,2′-bipyridyl)]Cl$_3$: ^{1}H NMR (DMSO) δ 13.95 (s, 2 H), 13.40 (s, 2 H), 8.76 (d, 2 H), 8.63 (m, 2 H), 8.46 (m, 8 H), 8.29 (d, 2 H), 7.84 (t, 4 H), 7.63 (t, 4 H), 2.39 (s, 6 H); FABMS 698 ([Rh(phi)$_2$(5,5′-dimethylbpy)]$^+$), 515 ([Rh(phi)$_2$]$^+$), 493 ([Rh(phi)(5,5′-dimethylbpy)]$^+$); extinction coefficient (ϵ) at λ = 350 nm, 21 600 M^{-1} cm^{-1}. Anal. Calcd (Found) for [Rh(phi)$_2$(5,5′-dimethylbpy)]Cl$_3$·6H$_2$O: C, 52.55 (51.2); N, 9.20 (8.7); H, 4.86 (4.5).

[Rh(phi)$_2$phen]Cl$_3$: ^{1}H NMR (DMSO) δ 13.95 (s, 2 H), 13.63 (s, 2 H), 9.12 (d, 2 H), 9.06 (d, 2 H), 8.69 (d, 2 H), 8.49 (m, 8 H), 8.23 (t, 2 H), 7.90 (t, 2 H), 7.84 (t, 2 H), 7.69 (t, 2 H), 7.58 (t, 2 H); FABMS 694 ([Rh(phi)$_2$phen]$^+$), 515 ([Rh(phi)$_2$]$^+$), 489 ([Rh(phi)(phen)]$^+$); extinction coefficient (ϵ) at λ = 350 nm is 22 000 M^{-1} cm^{-1}. Anal. Calcd (Found) for [Rh(phi)$_2$(phen)]Cl$_3$·6H$_2$O: C, 59.51 (58.7), H, 5.00 (4.5); N, 10.41 (10.10).

B. [Rh(2,2′-bipyridyl)$_2$phi]Cl$_3$ and Derivatives. The complex [Rh(bpy)$_2$phi]Cl$_3$ and its derivatives [Rh(4,4′-R$_2$-bpy)$_2$phi]Cl$_3$ (R = amido) and [Rh(5,5′-Me$_2$bpy)$_2$phi]Cl$_3$, as shown in Figure 1, were prepared according to the reported synthesis (Pyle et al., 1990a) of [Rh(phen)$_2$phi]Cl$_3$ and purified by cation-exchange chromatography (Sephadex CM C25, eluent 0.1–0.5 N HCl). The complex [Rh(4,4′-diphenyl-2,2′-bipyridyl)$_2$phi]Cl$_3$ was synthesized using an altered procedure. 4,4′-Diphenyl-2,2′-bipyridyl (0.61 g, 2.2 mmol) was dissolved in 700 μL of ethanol and added to a 5 mL aqueous mixture containing RhCl$_3$·6H$_2$O (0.26 g, 1 mmol) and hydrazine sulfate (0.2 mmol). After refluxing overnight, the reaction mixture was cooled on ice to promote the precipitation of [Rh(4,4′-diphenyl-2,2′-bipyridyl)$_2$Cl$_2$]Cl. The dichloro complex was washed with copious amounts of H$_2$O to remove unreacted RhCl$_3$·6H$_2$O and then converted to the bis(aquo) complex by adapting a literature procedure (Gideney et al., 1972). A solution of sodium hydroxide (2 M, 800 μL) was added to a suspension of 0.3 mmol of [Rh(4,4′-diphenyl-2,2′-bipyridyl)$_2$Cl$_2$]Cl in 20 mL of H$_2$O, and the alkaline mixture was boiled for 1 h. The reaction mixture was then neutralized with concentrated nitric acid, which promoted precipitation of the milky yellow [Rh(4,4′-diphenyl-2,2′-bipyridyl)$_2$(H$_2$O)$_2$]Cl$_3$ complex. The bis(aquo) complex was then dissolved in a mixture of 10 mL of DMF and 5 mL of isopropyl alcohol and the solution was thoroughly deaerated. A degassed solution of 9,10-diaminophenanthrene in 5 mL of ethanol was added to the solution containing [Rh(4,4′-diphenyl-2,2′-bipyridyl)$_2$(H$_2$O)$_2$]Cl$_3$. The reaction mixture was heated under an inert atmosphere at 65 °C for 24 h, and then air-oxidized for 24 h. Oxidation caused the deep red solution to turn milky orange, followed by precipitation of a brown-orange solid, which was resuspended in ethanol and air-oxidized for 24 h. The product [Rh(4,4′-diphenyl-2,2′-bipyridyl)$_2$(phi)]Cl$_3$ was purified by silica column chromotagraphy using a 3:2 mixture of ethyl acetate/ethanol as the eluent.

[Rh(2,2′-bipyridyl)$_2$(phi)]Cl$_3$: ^{1}H NMR (D$_2$O) 7.55 (t, 2 H), 7.6 (t, 2 H), 7.7 (d, 2 H), 7.75 (2 overlapping triplets, 4 H), 8.25 (2 overlapping triplets, 4 H), 8.35 (t, 2 H), 8.5 (t, 2 H), 8.55 (d, 2 H), 8.65 (d, 2 H), 8.72 (d, 2 H); UV–visible spectra maxima at 358, 313, and 301 nm; FABMS 609 ([Rh(bpy)$_2$phi – 2H]$^+$), 465 ([Rh(bpy)(phi)]$^+$), 415 ([Rh(bpy)$_2$]$^+$), 259 ([Rh(bpy)]$^+$); extinction coefficient (ϵ) at λ = 362 nm, 19 400 M^{-1} cm^{-1}. Anal. Calcd (Found) for [Rh(bpy)$_2$phi]Cl$_3$·12H$_2$O: C, 46.3 (45.81); H, 3.70 (3.71); N, 9.7 (9.20).

[Rh(4,4′-diphenyl-2,2′-bipyridyl)$_2$(phi)]Cl$_3$: ^{1}H NMR (D$_2$O) 7.43 (t, 2 H), 7.5 (m, 12 H), 7.7 (t, 2 H), 7.72 (d, 2 H), 7.8 (m, 6H), 7.85 (m, 4 H), 8.02 (d, 2 H), 8.16 (d, 4 H), 8.45 (d, 2 H), 8.92 (s, 2 H), 8.98 (s, 2 H) (the integrations correspond well with the expected values); UV–visible spectrum maximum at 272 nm; FABMS 925 ([Rh(DPB)$_2$phi]$^+$), 717 ([Rh(DPB)$_2$]$^+$), 617 ([Rh(DPB)(phi)]$^+$); extinction coefficient (ϵ) at λ = 362 nm, 47 000 M^{-1} cm^{-1}. Anal. Calcd (Found) for [Rh(4,4′-diphenylbpy)$_2$phi]Cl$_3$·6H$_2$O: C, 59.7 (58.7); H, 4.0 (3.8); N, 7.20 (6.98).

[Rh(4,4′-diamido-2,2′-bipyridyl)$_2$(phi)]Cl$_3$: ^{1}H NMR (D$_2$O) 7.38 (t, 2 H), 7.7 (t, 2 H), 7.8 (d, 2 H), 7.85 (d, 2 H), 8.1 (3 overlapping doublets, 6 H), 8.65 (d, 2 H), 9.00 (s, 2 H), 9.05 (s, 2 H); UV–visible spectrum maxima at 354, 325, 316 nm; FABMS 792 ([Rh(DAB)$_2$phi – H]$^+$), 552 ([Rh(DAB)phi]), 345 ([Rh(DAB)]$^+$), 588 ([Rh(DAB)$_2$]$^+$); extinction coefficient (ϵ) at λ = 362 nm, 17 500 M^{-1} cm^{-1}. Anal. Calcd (Found) for [Rh(4,4′-diamidobpy)$_2$phi]Cl$_3$·6H$_2$O: C, 43.2 (44.1); H, 3.4 (3.8); N, 13.2 (13.9).

[Rh(5,5′-dimethyl-2,2′-bipyridyl)$_2$(phi)]Cl$_3$: ^{1}H NMR (D$_2$O) the spectrum is sensitive to pH, addition of fumes of triflouroacetic acid sharpens the spectrum and improves the peak resolution, and the splitting pattern in a TFA-treated NMR sample is 2.0 (s, 2 H), 2.15 (s, 2 H), 7.15 (s, 2 H), 7.32 (t, 2 H), 7.62 (t, 2 H), 7.95 (d, 2 H), 8.05 (t, 6 H, 3 overlapping doublets), 8.29 (d, 2 H), 8.31 (d, 2 H); UV–visible spectra maxima at 360, 320, 314 nm; FABMS 675 ([Rh(DMB)$_2$phi – 2H]$^+$), 493 ([Rh(DMB)(phi)]$^+$), 287 ([Rh(DMB)]$^+$), 471 ([Rh(DMB)$_2$]$^+$); extinction coefficient (ϵ) at λ = 362 nm, 21 000 M^{-1} cm^{-1}. Anal. Calcd (Found) for [Rh(5,5′-dimethylbpy)$_2$phi]Cl$_3$·12H$_2$O: C, 48.98 (48.5); H, 4.64 (4.22); N, 9.78 (8.9).

C. Optical Resolution of [Rh(bpy)$_2$phi]Cl$_3$, [Rh(phen)$_2$phi]Cl$_3$, and [Rh(5,5′-dimethyl-2,2′-bipyridyl)$_2$phi]Cl$_3$. The Δ and Λ enantiomers of [Rh(phen)$_2$phi]Cl$_3$ were obtained as previously described (David & Barton, 1993). A modified version of this published procedure was used to resolve [Rh(bpy)$_2$phi]Cl$_3$ and [Rh(5,5′-dimethyl-2,2′-bipyridyl)$_2$phi]Cl$_3$. An aqueous solution containing 30 mg of racemic complex was loaded onto a Sephadex CM C25 column. The enantiomers were resolved into two well-separated red bands using a 0.1 M aqueous solution of tris(L-cysteinylsulfinato)cobaltate(III) ([Co(L-cysu)$_3$]$^{3-}$) as the chiral eluent (Cartwright et al., 1987). The column containing the two bands was then washed with 0.05 M KCl to replace the [Co(L-cysu)$_3$]$^{3-}$ anions with chlorides. The two bands were then eluted off the column using an aqueous solution of 0.3 M NaCl. CD spectra of the enantiomers were recorded in 50 mM sodium cacodylate buffer. The Δ isomers of [Rh(bpy)$_2$phi]Cl$_3$ at 318 nm ($\Delta\epsilon$ = –72 M^{-1} cm^{-1}) and of [Rh(5,5′-dimethyl-2,2′-bipyridyl)$_2$phi]Cl$_3$ at 329 nm ($\Delta\epsilon$ = –79 M^{-1} cm^{-1}) display negative circular dichroism. The absolute configurations were assigned on the basis of spectral similarity to [Rh(bpy)$_3$]Cl$_3$ (Dollimore & Gillard, 1989).

Photocleavage of DNA Restriction Fragments and Oligonucleotides. A 140 base pair 5′-[γ-^{32}P]- or 3′-[α-^{32}P]-labeled *Eco*RI/*Pvu*II fragment of pUC18 was prepared by standard methods. Cleavage reactions were carried out in 20 μL volumes contained in 0.65 mL siliconized Eppendorf tubes. Unless otherwise specified, reaction mixtures contained 65 μM nucleotide DNA (calf thymus or oligonucleotide substrate), labeled DNA, and 1 μM rhodium in 50 mM sodium

Table 1: DNA Sequence Selectivities[a] of $[Rh(phi)_2bpy]^{3+}$ and Its Derivatives

complex	sequence selectivity (5′→3′)[b]
$[Rh(phi)_2bpy]^{3+}$	A*T*GC, T*C*GT, A*C*GT, T*C*GC
$[Rh(phi)_2phen]^{3+}$	A*T*GC, T*C*GT, T*C*GC, C*C*CA
$[Rh(phi)_2(4,4'\text{-diamidobpy})]^{3+}$	A*T*GC, A*C*GG, T*C*AC, T*C*GT, T*C*GC
$[Rh(phi)_2(4,4'\text{-diphenylbpy})]^{3+}$	C*C*CA, C*C*AG, A*C*GC
$[Rh(phi)_2(5,5'\text{-dimethylbpy})]^{3+}$	C*C*CA, C*C*AG, A*G*TC, A*G*TG

[a] Sequence selectivities were obtained from the photocleavage patterns of $[Rh(phi)_2X]^{3+}$ complexes observed on restriction fragments derived from plasmid pUC18. Reaction mixtures containing 65 μM nucleotide and 1 μM Rh complex in 50 mM sodium cacodylate (pH 7.0) were irradiated at 310 nm for 8 min. [b] Primary sequence preference in a 5′→3′ direction, with cleavage occurring at the highlighted residue.

cacodylate buffer (pH 7.0). Reaction mixtures containing $[Rh(phi)_2]^{3+}$ complexes were irradiated for 20 min, while those containing $[Rh(phi)]^{3+}$ complexes were irradiated for 8 min.

After irradiations, the reaction mixtures containing restriction fragment as the DNA substrate were ethanol-precipitated with the addition of 10 μL of 7.5 M NH_4OAc and 60 μL of EtOH. The DNA pellets were washed with 200 μL of 80% ethanol, dried, and resuspended in 3 μL of loading buffer. The samples were then heat-denatured at 90 °C and quick-chilled on ice before loading onto a 8% denaturing polyacrylamide gel (Maniatis et al., 1982). Gels were electrophoresed at 1600 V for 2–3 h and dried at 70 °C for 1 h. The gels were transferred to a cassette and stored at −70 °C with Kodak X-Omat film.

RESULTS

Sequence Selectivities of $[Rh(phi)_2bpy]^{3+}$ *and Its Derivatives.* All of the derivatized $[Rh(phi)_2X]^{3+}$ complexes promote DNA strand scission with efficiencies comparable to that of $[Rh(phi)_2bpy]^{3+}$. The cleavage of supercoiled pUC18 DNA is similar in total efficiency for all of the $[Rh(phi)_2]^{3+}$ complexes, and HPLC as well as gel-electrophoretic analyses showed comparable extents of photocleavage of the oligonucleotide 5′-CTGGCATGCCAG-3′ by these complexes. A comparison of the sequence selectivities of these complexes was therefore made by examining their photocleavage patterns on restriction fragments. The hierarchy of sequence selectivities of each $[Rh(phi)_2X]^{3+}$ complex studied, as deduced from their photocleavage patterns on the *Pvu*II*/*Eco*RI fragment (Figure 2) and other restriction fragments (data not shown), is presented in Table 1. Although at concentrations ≥5 μM, $[Rh(phi)_2bpy]^{3+}$ may be regarded as sequence-neutral in its cleavage on DNA restriction fragments, at lower concentrations of rhodium, some site selectivity becomes evident (Figure 2). The parent complex $[Rh(phi)_2bpy]^{3+}$, as well as $[Rh(phi)_2phen]^{3+}$, shows a preference for some 5′-*py*-pu-3′ and 5′-*py*-py-3′ sequences, with cleavage occurring at the highlighted pyrimidine. The complexes $[Rh(phi)_2(4,4'\text{-diamidobpy})]^{3+}$, $[Rh(phi)_2(5,5'\text{-dimethylbpy})]^{3+}$, and $[Rh(phi)_2(4,4'\text{-diphenylbpy})]^{3+}$ generally cleave at a smaller subset of sites recognized by the parent complex; however, $[Rh(phi)_2(5,5'\text{-dimethylbpy})]^{3+}$ also cleaves at the guanine of 5′-A*G*T sequences that are not cleaved by the parent $[Rh(phi)_2bpy]^{3+}$ complex. The subset of cleavage sites, noteworthy for example at 5′-C*C*CA-3′ and 5′-T*C*GT-3′, appears to reflect a reduction in cleavage, perhaps as a result of steric considerations, compared to the parent complex; generally, a loss of cleavage by these complexes is apparent at sites containing a 5′-purine.

Sequence Selectivities of $[Rh(bpy)_2phi]^{3+}$ *and Its Derivatives.* The sequence selectivities and asymmetry in DNA

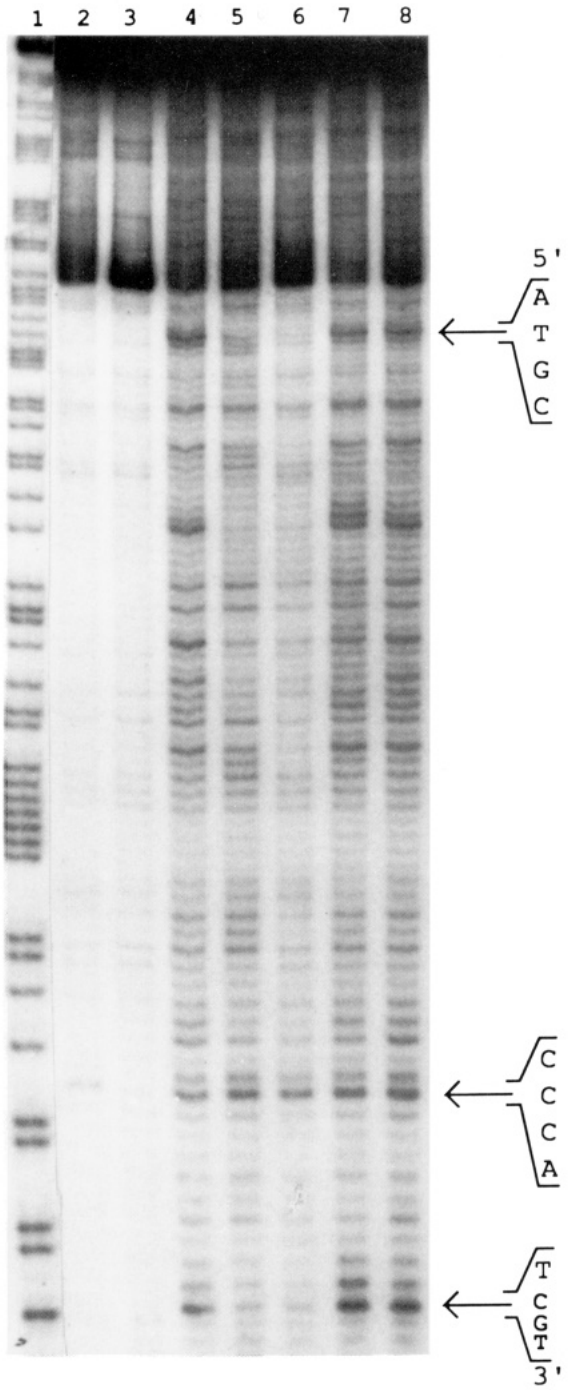

FIGURE 2: Sequence-specific recognition of DNA by $[Rh(phi)_2bpy]^{3+}$ and its derivative complexes: importance of steric interactions. Autoradiogram of an 8% polyacrylamide gel after photocleavage of a 3′-^{32}P-end-labeled *Pvu*II/*Eco*RI fragment of pUC18: lane 1, Maxam–Gilbert A+G reaction; lane 2, untreated fragment; lane 3, fragment irradiated in the absence of rhodium complex; lanes 4–8, 3′-^{32}P-end-labeled fragments irradiated in the presence of 1 μM $[Rh(phi)_2bpy]^{3+}$, $[Rh(phi)_2(5,5'\text{-dimethylbpy})]^{3+}$, $[Rh(phi)_2(4,4'\text{-diphenylbpy})]^{3+}$, $[Rh(phi)_2(4,4'\text{-diamidobpy})]^{3+}$, and $[Rh(phi)_2phen]^{3+}$, respectively. The complexes $[Rh(phi)_2bpy]^{3+}$ (lane 4), $[Rh(phi)_2(4,4'\text{-diamidobpy})]^{3+}$ (lane 7), and $[Rh(phi)_2phen]^{3+}$ (lane 8) cleave at most sites, but show a moderate preference for the 5′-A*T*GC-3′, 5′-C*C*CA-3′, and 5′-T*C*GT-3′ sequences (marked with arrows), with cleavage occurring at the highlighted residues. The complexes $[Rh(phi)_2(5,5'\text{-dimethylbpy})]^{3+}$ (lane 5) and $[Rh(phi)_2(4,4'\text{-diphenylbpy})]^{3+}$ (lane 6) cleave preferentially only at the 5′-CCCA-3′ sequence. These data illustrate that additional steric interactions introduced by appropriately positioned methyl and phenyl groups make these complexes more selective toward sequence-dependent DNA structures.

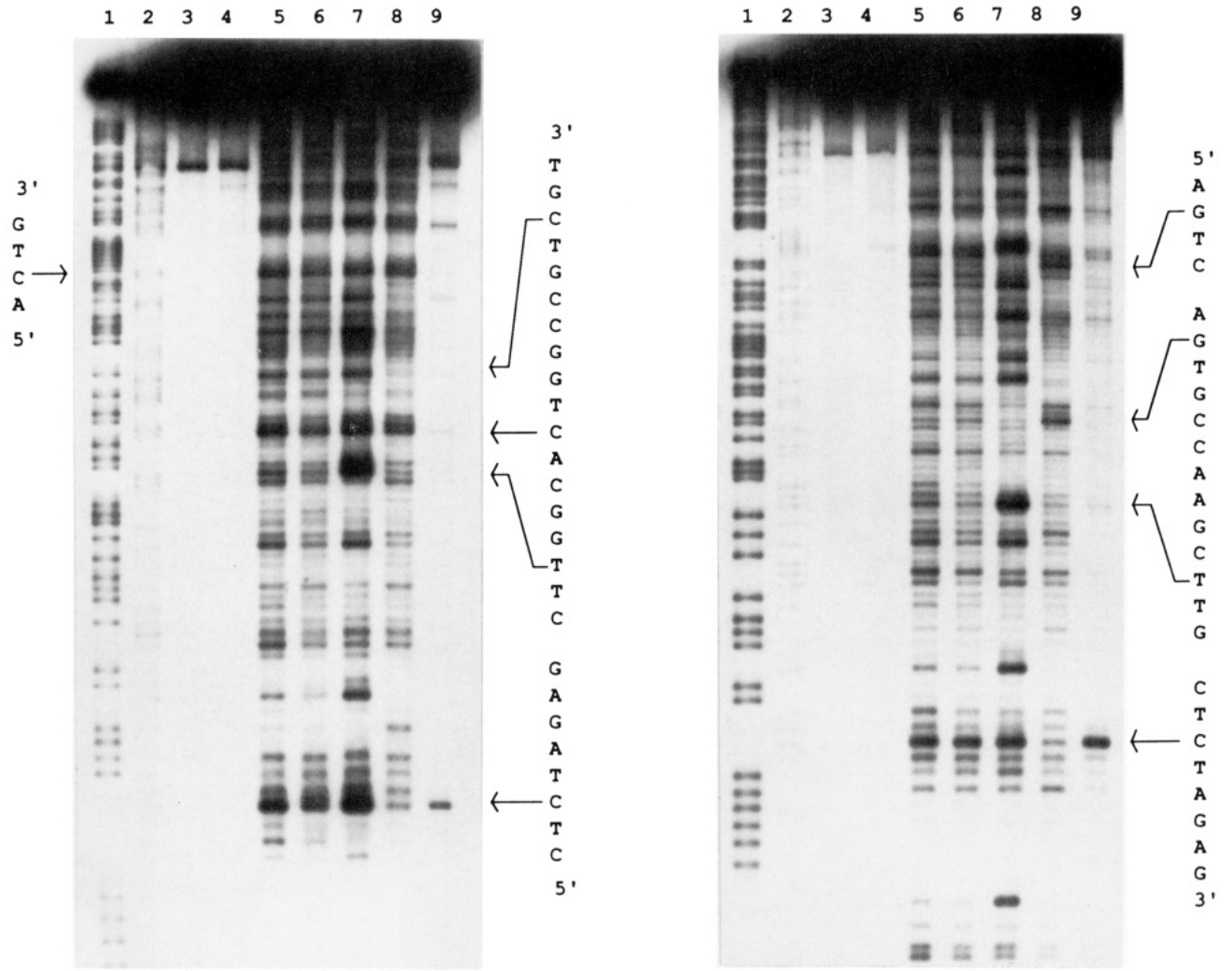

FIGURE 3: Sequence-specific recognition of DNA by $[Rh(bpy)_2phi]^{3+}$ and its derivative complexes. Autoradiogram of an 8% polyacrylamide gel after photocleavage of 5′-^{32}P- (left) and 3′-^{32}P-(right) end-labeled *Eco*RI/*Pvu*II fragments of pUC18: lanes 1 and 2, Maxam–Gilbert A+G and C+T reactions; lane 3, untreated fragment; lane 4, fragment irradiated in the absence of rhodium complex; lanes 5–9, 5′-^{32}P- or 3′-^{32}P-end-labeled fragments irradiated in the presence of 1 μM $[Rh(bpy)_2phi]^{3+}$, $[Rh(phen)_2phi]^{3+}$, $[Rh(4,4'\text{-diamidobpy})_2phi]^{3+}$, $[Rh(5,5'\text{-dimethylbpy})_2phi]^{3+}$, and $[Rh(4,4'\text{-diphenylbpy})_2phi]^{3+}$, respectively.

cleavage by the $[Rh(phi)]^{3+}$ series of complexes was also studied by examining their photocleavage patterns on 5′-^{32}P- and 3′-^{32}P-end-labeled restriction fragments. Again, $[Rh(phi)]^{3+}$ complexes cleave supercoiled plasmids upon photoactivation with efficiencies comparable to that of $[Rh(phen)_2phi]^{3+}$; however, under identical reaction conditions, their sequence selectivities differ markedly. The photocleavage reactions were carried out at low concentrations (≤ 1 μM) of metal complex to ascertain their sequence selectivities. As shown in Figure 3, all of the complexes show site selectivity in cleavage on the restriction fragment. Furthermore, compared to the $[Rh(phi)_2]^{3+}$ complexes (Figure 2), the $[Rh(phi)]^{3+}$ complexes show significantly greater specificity. The complexes $[Rh(bpy)_2phi]^{3+}$ and $[Rh(phen)_2phi]^{3+}$ have similar photocleavage patterns and cleave preferentially at 5′-py-*py*-py-3′ and 5′-py-*py*-pu-3′ base steps, with cleavage occurring at the highlighted pyrimidine. The complex $[Rh(4,4'\text{-diamidobpy})_2phi]^{3+}$ cleaves at sequences that are also recognized by the parent complex; however, its affinity toward some sites is increased significantly, possibly as a result of hydrogen-bonding contacts between its amido groups and the DNA–phosphate backbone. Owing to the steric demands imposed by methyl and phenyl moieties, the complexes $[Rh(5,5'\text{-dimethylbpy})_2phi]^{3+}$ and $[Rh(4,4'\text{-diphenylbpy})_2phi]^{3+}$ show cleavage at only a small subset of sites cleaved by the parent $[Rh(bpy)_2phi]^{3+}$. While $[Rh(5,5'\text{-dimethylbpy})_2phi]^{3+}$ cleaves strongly at 5′-A*C*TG-3′ and 5′-A*G*TC-3′ sites, $[Rh(4,4'\text{-diphenylbpy})_2phi]^{3+}$ is highly specific for the two 5′-CTCTAG-3′ sites on opposing strands contained in the palindromic 5′-CTCTAGAG-3′ sequence. A summary of the sites targeted by the $[Rh(phi)X_2]^{3+}$ complexes is illustrated as a histogram in Figure 4.

Owing to the high level of specific cleavage induced by $[Rh(phi)]^{3+}$ complexes, the 5′-asymmetry in their cleavage patterns can be seen by comparing their cleavage patterns on the 5′-^{32}P- and 3′-^{32}P-end labeled *Eco*RI*/*Pvu*II 144 bp fragment. In general, cleavage at sites containing a central 5′-*py*-py-3′ base step occurs only on the pyrimidine strand, with no corresponding cleavage observed in a 5′-direction at the 5′-*pu*-pu-3′ step of the opposing strand. However, as shown in the histograms in Figure 4, cleavage at some 5′-*py*-pu-3′ base steps is associated with 5′-asymmetric cleavage at the complementary 5′-*py*-pu-3′ base step on the opposing strand. For example, cleavage at 5′-T*T*GG-3′ is associated with 5′-asymmetric cleavage at 5′-C*C*AA-3′, and cleavage at 5′-A*C*AA-3′ is associated with 5′-asymmetric cleavage at T*T*GT. These results are consistent with binding from the major groove (Sluka et al., 1987) and suggest that the complex is more symmetrically bound in the helix at 5′-py-pu-3′ steps than at 5′-py-py-3′ sites.

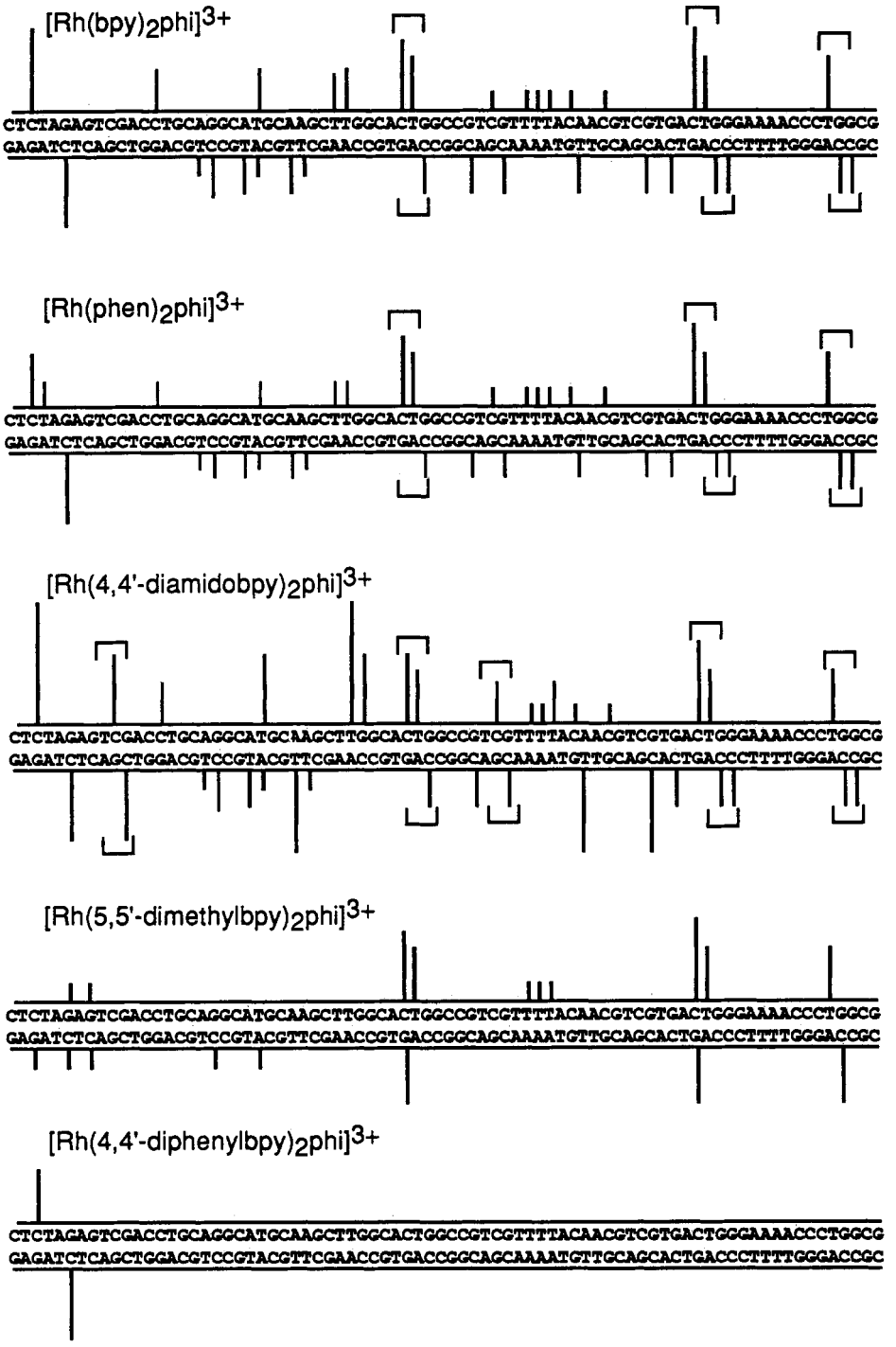

FIGURE 4: Comparison of DNA photocleavage by $[Rh(phi)X_2]^{3+}$ complexes. Histogram illustrating the relative cleavage by the complexes $[Rh(bpy)_2phi]^{3+}$, $[Rh(phen)_2phi]^{3+}$, $[Rh(4,4'\text{-diamidobpy})_2phi]^{3+}$, $[Rh(5,5'\text{-dimethylbpy})_2phi]^{3+}$, and $[Rh(4,4'\text{-diphenylbpy})_2phi]^{3+}$ at sites along the 5'-labeled (top) and 3'-labeled (bottom) *Eco*RI/*Pvu*II fragments of pUC18.

Sequence Selectivities of the Δ and Λ Enantiomers of $[Rh(bpy)_2phi]^{3+}$, $[Rh(phen)_2phi]^{3+}$, and $[Rh(5,5'\text{-dimethylbpy})_2phi]^{3+}$. To better understand the basis for sequence selectivity by these complexes, it is essential to distinguish the sequence preferences of Δ and Λ isomers. Previous work has shown that the complex $[Rh(phen)_2phi]^{3+}$ binds enantioselectively at 5'-py-pu-3' base steps. While the Δ isomer of this complex cleaves specifically at the py of 5'-*py*-pu steps, the Λ isomer shows no corresponding cleavage at these steps (Pyle et al., 1990b; Campisi et al., 1994). As shown in Figure 5, we compared the photocleavage patterns of the enantiomers of $[Rh(bpy)_2phi]^{3+}$, $[Rh(phen)_2phi]^{3+}$, and $[Rh(5,5'\text{-dimethylbpy})_2phi]^{3+}$ on the 5'-^{32}P- and 3'-^{32}P-end-labeled *Eco*RI*/*Pvu*II 144 base pair fragment from plasmid pUC18. The photocleavage experiment was carried out at low concentrations of each metal complex (0.2 μM) so as to differentiate clearly between strong sites recognized by their respective Δ and Λ isomers. Isomers of $[Rh(bpy)_2phi]^{3+}$ and $[Rh(phen)_2phi]^{3+}$ show very similar recognition patterns. The Δ isomers of both complexes cleave strongly at both 5'-py-py and 5'-pu-pu base steps, while the Λ isomers have no strong sites. In comparison, the Δ and Λ isomers of $[Rh(5,5'\text{-dimethylbpy})_2phi]^{3+}$ each have distinctly different recognition sequences. While the Δ isomer cleaves strongly at 5'-C*T*TG-3' and 5'-C*A*TG-3' sites, the Λ isomer cleaves strongly at 5'-A*C*TG-3', 5'-A*G*TG-3', and 5'-A*G*TC-3' sites. This

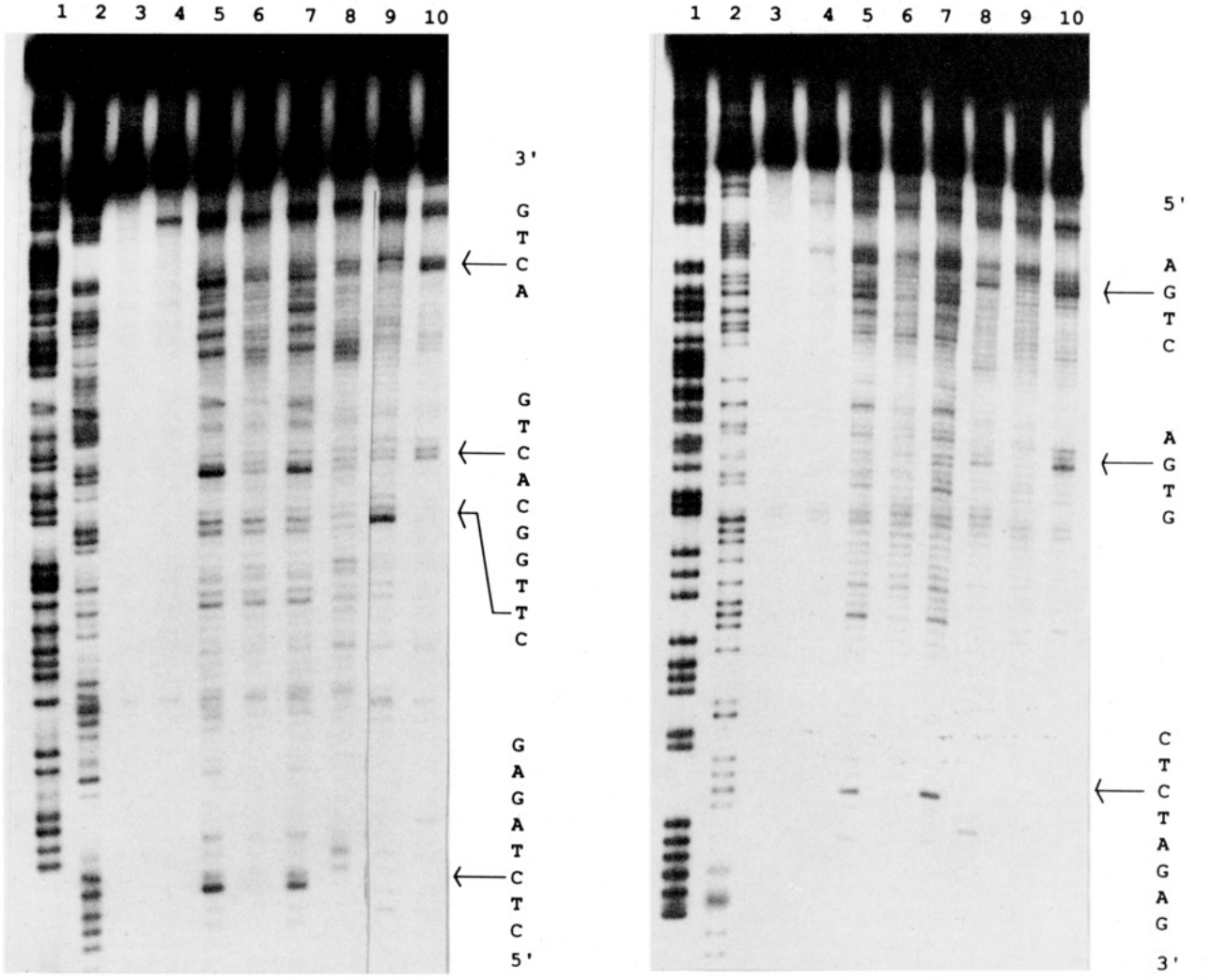

FIGURE 5: Enantioselectivity in DNA sequence recognition by the Δ and Λ isomers of $[Rh(bpy)_2phi]^{3+}$, $[Rh(phen)_2phi]^{3+}$, and $[Rh(5,5'\text{-dimethylbpy})_2phi]^{3+}$. Autoradiogram of an 8% polyacrylamide gel after photocleavage of 5′-^{32}P- (left) and 3′-^{32}P- (right) end-labeled *Eco*RI/*Pvu*II fragments of pUC18: lanes 1 and 2, Maxam–Gilbert A+G and C+T reactions; lane 3, untreated fragment; lane 4, fragment irradiated in the absence of rhodium complex; lanes 5–10, 5′-^{32}P- or 3′-^{32}P- end-labeled fragments irradiated in the presence of 0.2 μM Δ-$[Rh(bpy)_2phi]^{3+}$, Λ-$[Rh(bpy)_2phi]^{3+}$, Δ-$[Rh(phen)_2phi]^{3+}$, Λ-$[Rh(phen)_2phi]^{3+}$, Δ-$[Rh(5,5'\text{-dimethylbpy})_2phi]^{3+}$, and Λ- $[Rh(5,5'\text{-dimethylbpy})_2phi]^{3+}$, respectively. Note that the cleavage patterns by the Δ and Λ isomers of $[Rh(bpy)_2phi]^{3+}$ and $[Rh(phen)_2phi]^{3+}$ are very similar; the Δ isomers of both complexes cleave strongly at the 5′-T*C*TA-3′ and 5′-A*C*TG-3′ sequences, while the corresponding Λ isomers have no strong sites of cleavage. In comparison, the Δ isomer of $[Rh(5,5'\text{-dimethylbpy})_2phi]^{3+}$ cleaves strongly at the 5′-C*T*TG-3′ sequence, while the Λ isomer cleaves strongly at the 5′-A*C*TG-3′, 5′-A*G*TG-3′, and 5′-A*G*TC-3′ sequences.

comparison points to the *importance of both steric clashes and methyl–methyl van der Waals interactions* in enhancing the sequence specificity of $[Rh(phi)]^{3+}$ complexes. A summary of preferred sites of cleavage by the Δ and Λ isomers of the three complexes studied is presented in Table 2.

Table 2: Sequence Selectivities[a] of the Δ and Λ Isomers of $[Rh(bpy)_2phi]^{3+}$, $[Rh(phen)_2phi]^{3+}$, and $[Rh(5,5'\text{-dimethylbpy})_2phi]^{3+}$

	sequence selectivity[b]	
complex	Δ enantiomer	Λ enantiomer
$[Rh(bpy)_2phi]^{3+}$	T*C*TA (s), C*T*TG (s), A*C*TG (s)	A*C*TG (w)
$[Rh(phen)_2phi]^{3+}$	T*C*TA (s), C*T*TG (s), A*C*TG (s)	A*C*TG (w)
$[Rh(5,5'\text{-dimethylbpy})_2phi]^{3+}$	C*T*TG (s), C*A*TG (s)	A*C*TG (s), A*G*TG (s), A*G*TC (s)
consensus sequence	C*N*TG	A*C*/*G*TC/G

[a] The reaction mixtures, containing 65 μM nucleotide and 0.2 μM Rh complex (Δ or Λ isomer) in 50 mM sodium cacodylate (pH 7.0), were irradiated at 310 nm for 8 min. [b] All sequences are written in a 5′→3′ direction. Cleavage is observed at the highlighted residue in the recognition sequences. The strong sites are labeled (s) and weaker sites (w).

DISCUSSION

Common Characteristics of the Rhodium Complexes. On the basis of similarities in recognition and reaction of the derivative complexes to the parents $[Rh(phen)_2phi]^{3+}$ and $[Rh(phi)_2bpy]^{3+}$, these complexes all appear to bind tightly in the major groove of DNA through intercalation of the phi ligand. The complexes show equivalent efficiencies and products of photoreaction with DNA, where the products are consistent with abstraction of the C3′-hydrogen atom and subsequent degradation, which depends upon access of the C3′-radical to dioxygen; the reactivity therefore is sensitively dependent upon shape recognition (Sitlani et al., 1992). The differences in sites of photoreaction may therefore be applied in comparing DNA recognition characteristics. A direct correlation between photocleavage and binding sites, detected through DNA footprinting, has been observed for $[Rh(diphenylbpy)_2phi]^{3+}$ (Sitlani et al., 1993), the most selective complex examined thus far. The $[Rh(phi)]^{3+}$ complexes also show 5′-asymmetry in cleavage, an indication that access is,

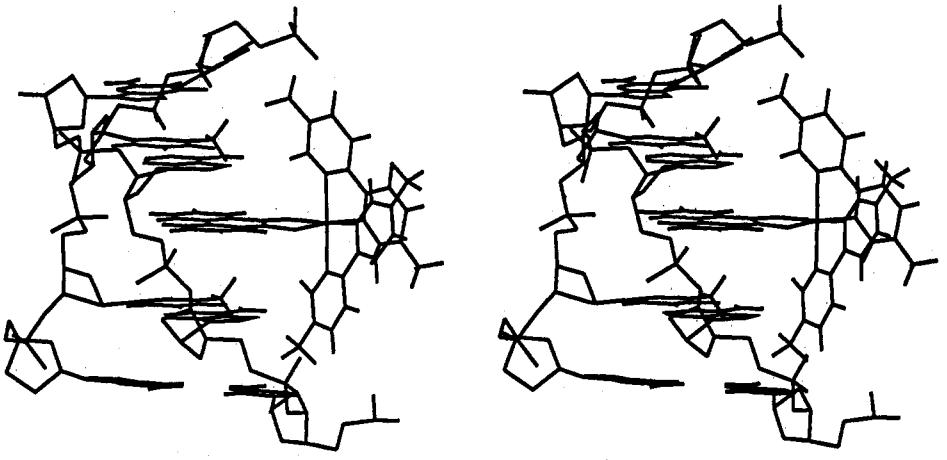

FIGURE 6: Stereoview of a model of Δ-[Rh(5,5′-dimethylbpy)$_2$phi]$^{3+}$ (right) intercalated in the duplex 5′-CTTG-3′ (left). Note the shape complementarity of the complex bound in the site to the DNA helix, as well as the positioning of the methyl groups on the ancillary ligands of the complex for stabilizing contacts with the methyl groups of the internal thymines.

in general, from the DNA major groove (Sluka et al., 1987). Differences in site recognition are apparent, however, as a function of substitution on the ancillary nonintercalating ligands. Hence, derivatization of phi complexes of rhodium offers an attractive strategy to construct an array of DNA-binding molecules.

Recognition Characteristics of [Rh(phi)$_2$X]$^{3+}$ Complexes. Steric interactions appear to dominate the sequence selectivities of the [Rh(phi)$_2$X]$^{3+}$ complexes. Specifically, introduction of hydrophobic residues such as methyl groups in the 5,5′-positions or phenyl groups in the 4,4′-positions of the ancillary bipyridyl ligand significantly *restricts* the DNA sites targeted by these complexes. The net result is an apparent increase in site selectivity for the derivative complexes [Rh(phi)$_2$(5,5′-dimethylbpy)]$^{3+}$ and [Rh(phi)$_2$(4,4′-diphenylbpy)]$^{3+}$ compared to their parent complex [Rh(phi)$_2$bpy]$^{3+}$. Thus, the steric demands imposed by the bulky ancillary ligands of these complexes diminish their binding affinity to most sequences and thereby enhance their overall sequence specificities. Since these complexes bind tightly to DNA ($K_a \geq 10^6$ M^{-1}), their relative binding to different DNA sequences therefore can be modulated by steric interactions. Thus, by adding a bulky functionality, we may construct a complex of significantly higher site selectivity from a sequence-neutral one.

The shapes of [Rh(phi)$_2$X]$^{3+}$ complexes clearly determine their overall DNA recognition properties. However, for these complexes the specific structural considerations behind their individual sequence selectivities is not clearly apparent. A comparison of the sequence selectivities of the [Rh(phi)$_2$X]$^{3+}$ complexes (Table 1) indicates that there is no consensus sequence describing their selectivities. This observation is not surprising, since [Rh(phi)$_2$X]$^{3+}$ complexes lack a C_2 axis of symmetry about their intercalating phi ligand. Therefore, racemic mixtures of each [Rh(phi)$_2$X]$^{3+}$ complex should have four distinct intercalatively bound species (two derived from intercalation by each of the two phi ligands and the other two from their Δ and Λ isomers), each of which would likely have its own distinct sequence selectivity.

Recognition Characteristics of [Rh(phi)X$_2$]$^{3+}$ Complexes. In comparison to the [Rh(phi)$_2$X]$^{3+}$ complexes, the [Rh(phi)X$_2$]$^{3+}$ complexes do cleave DNA at specific sites that may be defined by consensus sequences. The [Rh(phi)X$_2$]$^{3+}$ complexes are C_2-symmetric about their single intercalating phi ligand, which contributes to their greater sequence specificity compared to the [Rh(phi)$_2$X]$^{3+}$ complexes. Furthermore, the nonintercalating ligands in the [Rh(phi)X$_2$]$^{3+}$ complexes are in close proximity to the DNA helix, making them sensitive probes to variations in sequence-dependent structure. Steric and van der Waals interactions dominate the overall DNA specificities of [Rh(phi)X$_2$]$^{3+}$ complexes. It is noteworthy that the phenyl functionalities, which are substituted on the 4,4′-positions of the nonintercalating ligands, are directed toward the DNA backbone and may be less direct sensors of sequence-dependent local structure than the 5,5′-methyl functionalities, which are pointed instead toward the DNA base pairs. In the one case examined here, hydrogen-bonding contacts appear to enhance DNA affinity, but not specificity. This observation may not be a general reflection of the consequence of introducing hydrogen-bonding groups, but certainly in the absence of highly specific contacts, hydrogen bonding to the phosphate backbone would be expected to yield increased overall affinity but not specificity. Thus, while the complex [Rh(4,4′-diamidobpy)$_2$phi]$^{3+}$ cleaves more strongly at sites recognized by [Rh(bpy)$_2$phi]$^{3+}$, the complexes [Rh(4,4′-diphenylbpy)$_2$phi]$^{3+}$ and [Rh(5,5′-dimethylbpy)$_2$phi]$^{3+}$ cleave at a small subset of sites recognized by the parent complex. Remarkably, the bulky complex [Rh(4,4′-diphenylbpy)$_2$phi]$^{3+}$ is highly specific for the palindromic sequence 5′-CTCTAGAG-3′. This specificity is derived in part from shape selection, but also from the facility of the complex to dimerize noncovalently on this palindromic sequence (Sitlani et al., 1993).

The importance of specific van der Waals methyl–methyl interactions in governing DNA recognition is illustrated in the enantioselective cleavage by [Rh(5,5′-dimethylbpy)$_2$phi]$^{3+}$. The Δ isomer cleaves strongly at the 5′-C*T*TG-3′ site, while the Λ isomer cleaves strongly at 5′-A*C*TG-3′ and 5′-A*G*T-3′ sites. These differing site selectivities may be understood in viewing the complexes bound to the different double-helical sequences in three dimensions. Molecular modeling studies predict that the Δ isomer would preferentially bind to 5′-C$_1$*T*$_2$T$_3$G$_4$-3′ and 5′-C$_1$*T*$_2$G$_3$G$_4$-3′ sites with the thymine methyl groups (at positions 2 and/or 3) located at 4 Å van der Waals distances from the 5,5′-methyl groups of the intercalated Δ-[Rh(5,5′-dimethylbpy)$_2$phi]$^{3+}$. Figure 6 illustrates this interaction as well as the shape and symmetry complementarity of the metal complex bound in this site. Modeling studies, for example, also indicate that this isomer cannot bind to sites with sequences of the type 5′-T$_1$N$_2$N$_3$A$_4$-3′ (N = py/pu) due to strong steric clashes between the thymine methyl groups (at positions 1 and 4) and the 5,5′-methyl groups of the intercalated complex. Conversely, the thymine methyl

groups at positions 1 and 4 of sequence 5′-$A_1N_2N_3T_4$-3′ are far enough from the methyl groups of the intercalated complex such that they neither introduce steric clashes nor afford positive van der Waals contacts. Hence, consistent with this modeling, the cleavage data indicate that the Δ isomer cleaves strongly at 5′-C*T*TG-3′ sequences but more moderately at 5′-C*T*GG-3′ sequences. However, the Δ isomer also cleaves strongly at 5′-$C_1A_2T_3G_4$-3′, suggesting that a thymine at position 3 is more important than one at position 2. Similarly, molecular modeling studies show that the Λ isomer would preferentially bind to 5′-$A_1N_2T_3N_4$-3′ sequences, with the thymine methyls in positions 1 and 3 located at van der Waals distances from the 5,5′-methyls of the Λ isomer. Consistent with these predictions, the Λ isomer cleaves at 5′-A*C*TG-3′ and 5′-A*G*T-3′ sequences. Not surprisingly, then, the two enantiomers target distinctly different sequences.

A comparison of the DNA sequence selectivities of the isomers for the series $[Rh(bpy)_2phi]^{3+}$, $[Rh(phen)_2phi]^{3+}$, and $[Rh(5,5'\text{-dimethylbpy})_2phi]^{3+}$ shows that the 5,5′-methyl groups on the ancillary ligands of $[Rh(5,5'\text{-dimethylbpy})_2phi]^{3+}$ enhance both binding affinity and chiral discrimination. For $[Rh(phen)_2phi]^{3+}$ and $[Rh(bpy)_2phi]^{3+}$, only their Δ enantiomers cleave at the preferred 5′-py-py-3′ and 5′-py-pu-3′ sites, with little cleavage induced by their corresponding Λ enantiomers. Furthermore, as shown earlier (Sitlani et al., 1993), only the Δ isomer and not the Λ isomer of $[Rh(4,4'\text{-diphenylbpy})_2phi]^{3+}$ binds and cleaves specifically at the 8 base pair 5′-CTCTAGAG-3′ site. In comparison, *both* the Δ and Λ enantiomers of $[Rh(5,5'\text{-dimethylbpy})_2phi]^{3+}$ show strong sequence selectivities for DNA, with each enantiomer having its own set of preferred sites. Specifically, Δ-$[Rh(5,5'\text{-dimethylbpy})_2phi]^{3+}$ mainly binds at a subset of sites recognized by the Δ isomers of $[Rh(bpy)_2phi]^{3+}$ and $[Rh(phen)_2phi]^{3+}$, owing to the additional steric demands imposed by its ancillary 5,5′-dimethyl groups. This example underscores how *negative* steric clashes can increase the sequence specificity of $[Rh(phi)]^{3+}$ complexes. In comparison, Λ-$[Rh(5,5'\text{-dimethylbpy})_2phi]^{3+}$ is strongly enantioselective for 5′-AGT and 5′-ACT sites, which correspondingly are not recognized by the Λ isomers of $[Rh(phen)_2phi]^{3+}$ and $[Rh(bpy)_2phi]^{3+}$. This example may illustrate how *stabilizing* interactions between the methyl groups on the complex and the thymine methyl groups in DNA may enhance the binding affinity and therefore the specificity of the Λ isomer for certain DNA sequences. A similar stabilizing interaction based upon methyl–methyl contacts with thymine has been demonstrated in DNA recognition by Λ-$[Rh(ethylenediamine)_2phi]^{3+}$ (Krotz et al., 1993a). The added stabilization in these systems appears to be on the order of 1 kcal/mol for the methyl–methyl interaction (Krotz et al., 1993a,b; Plaxco, 1994), and a similar stabilization is evident on the basis of the comparison of cleavage efficiencies for $[Rh(5,5'\text{-dimethylbpy})_2phi]^{3+}$ and $[Rh(bpy)_2phi]^{3+}$.

Implications for New Design. As we have seen earlier with different transition metal complexes (Chow & Barton, 1992), this examination of $[Rh(phi)]^{3+}$ complexes with DNA illustrates how steric interactions may dominate sequence-selective recognition. The complementarity between the shapes of these rhodium intercalators and DNA primarily governs the ability of these complexes to detect sequence-dependent DNA structure. The more sterically bulky complexes with methyl or phenyl groups on their ancillary bipyridyl ligands show the highest sequence specificities. Most of the derivative complexes bind selectively at *a subset of sequences* recognized by their respective parent complexes. Importantly, however, the derivative complexes $[Rh(5,5'\text{-dimethylbpy})_2phi]^{3+}$ and $[Rh(phi)_2(5,5'\text{-dimethylbpy})]^{3+}$ also target 5′-AGT-3′ sequences, which are *not* selectively targeted by their respective parent complexes. This new site preference, compared to the parent complex, points to the importance of specific van der Waals interactions between methyl groups on the intercalated metal complex and methyl groups on DNA in enhancing sequence-specific recognition by these metal complexes. Like these rhodium complexes, DNA-binding proteins, which bind in the major groove, may similarly employ an ensemble of steric and van der Waals interactions to discriminate between sequences. The application of steric constraints to achieve site specificity in a predictive manner is difficult at this stage, since our knowledge of local sequence-dependent DNA structure is still only rudimentary. Augmentation of site specificity through the careful introduction of stabilizing methyl–methyl interactions does, however, offer a route to some measure of predictive design. Certainly both steric interactions and methyl–methyl van der Waals interactions should play critical roles in the rational design of new DNA-targeted chemotherapeutics.

ACKNOWLEDGMENT

We thank A. M. Pyle for her syntheses of several $Rh(phi)_2^{3+}$ complexes.

REFERENCES

Badger, G. H., & Sasse, W. H. F. (1956) *J. Am. Chem. Soc. 78*, 616.
Campisi, D., Morii, T., & Barton, J. K. (1994) *Biochemistry 33*, 4130.
Cartwright, P. S., Gillard, R. D., & Sillanpaa, E. R. J. (1987) *Polyhedron 6*, 105.
Chow, C. S., & Barton, J. K. (1992) *Methods Enzymol. 212*, 219.
David, S., & Barton, J. K. (1993) *J. Am. Chem. Soc. 115*, 2984.
Dollimore, L. S., & Gillard, R. D. (1989) *Polyhedron 8*, 1163.
Evers, R. C., & Moore, G. J. (1986) *J. Polym. Sci. Part A 24*, 1873.
Gideney, P. M., Gillard, R. D., & Heaton, B. T. (1972) *J. Chem. Soc., Dalton Trans.*, 2621.
Howells, R. D., & McCown, J. D. (1977) *Chem. Rev. 77*, 69.
Krotz, A. H., Kuo, L. Y., Shields, T. P., & Barton, J. K. (1993a) *J. Am. Chem. Soc. 115*, 3877–3882
Krotz, A. H., Hudson, B. P., & Barton, J. K. (1993b) *J. Am. Chem. Soc. 115*, 12577–12578.
Maniatis, T., Fritsch, E. F., & Sambrook, J. (1982) *Molecular Cloning*, Cold Spring Harbor Laboratory Press, Cold Spring Harbor, NY.
Plaxco, R. (1994) *Biochemistry 33*, 3050.
Pyle, A. M., & Barton, J. K. (1990) *Prog. Inorg. Chem. 38*, 413.
Pyle, A. M., Long, E. C., & Barton, J. K. (1989a) *J. Am. Chem. Soc. 111*, 4520.
Pyle, A. M., Rehmann, J. P., Meshoyrer, R., Kumar, C. V., Turro, N. J., & Barton, J. K. (1989b) *J. Am. Chem. Soc. 111*, 3051.
Pyle, A. M., Chiang, M. Y., & Barton, J. K. (1990a) *Inorg. Chem. 29*, 4487.
Pyle, A. M., Morii, T., & Barton, J. K. (1990b) *J. Am. Chem. Soc. 112*, 9432.
Sitlani, A., Long, E. C., Pyle, A. M., & Barton, J. K. (1992) *J. Am. Chem. Soc. 114*, 2303.
Sitlani, A., Dupureur, C. M., & Barton, J. K. (1993) *J. Am. Chem. Soc. 115*, 12589–90.
Sluka, J. P., Horvath, S. J., Bruist, M. F., Simon, M. I., & Dervan, P. B. (1987) *Science 238*, 1129.